# Medium-energy hadron-nucleus scattering in the $1/N$ expansion formalism

S. Kuyucak
*Department of Theoretical Physics, Research School of Physical Sciences, Australian National University, Canberra, ACT 0200, Australia*

I. Morrison
*School of Physics, University of Melbourne, Parkville, Victoria 3052, Australia*

(Received 22 July 1992)

The algebraic-eikonal approach to the medium-energy hadron-nucleus scattering is generalized to arbitrary interactions and boson types using the $1/N$ expansion technique for the interacting boson model. The results are used in a comparative study of proton scattering from deformed nuclei in the *sd* and *sdg* boson models. The two models give almost identical results for a pure quadrupole interaction but widely differ when a hexadecapole interaction is included.

PACS number(s): 24.10.Eq, 25.40.Ep, 21.60.Ev

## I. INTRODUCTION

Medium-energy proton-nucleus scattering experiments have demonstrated that the distorted-wave impulse approximation breaks down at high momentum transfers and multiple scattering effects must be included for a proper description of data [1]. The traditional coupled-channel calculations give improved agreement, however, they are time consuming and not very illuminating. An alternative approach pioneered by Amado, Dedonder, and Lenz [2] is to use the eikonal approximation [3] which leads to analytic expressions for scattering cross sections, and provides valuable insight into these processes (see [4] for a review).

Recently, Ginocchio *et al.* [5] combined the eikonal approximation with the interacting boson model (IBM) [6] opening the way for a unified description of hadron scattering from collective nuclei. In the initial work [5], the U(5), O(6), and SU(3) dynamical symmetries of the IBM were exploited to obtain closed analytic expressions for the transition matrix elements. As the dynamical symmetries are not realized in majority of nuclei, realistic applications of the model [7–9] still had to be done numerically, e.g., diagonalization of the IBM Hamiltonian and calculation of various matrix elements.

The IBM with $s$ and $d$ bosons gives an adequate description of the quadrupole properties of low-lying levels. Recent electron [10] and proton [11] scattering experiments have shown, however, that this success does not extend to the $E4$ properties. This and other shortcomings of the *sd* IBM [e.g., existence of $K=3^+$ and $4^+$ bands, lack of boson cutoff in $B(E2)$ values] can be resolved in the *sdg* model as demonstrated by calculations in deformed [12] and transitional [13] nuclei. Clearly, it is desirable to extend the above eikonal+IBM calculations to the *sdg* model especially in the case of $J=4^+$ states. Numerical implementation of such a calculation, however, is rather difficult due to the much larger *sdg* basis space.

The $1/N$ expansion [14,15] provides approximate analytic solutions for general IBM Hamiltonians with arbitrary kinds of bosons, and is particularly useful in cases where numerical diagonalization is not practical because of large basis spaces. The purpose of this paper is to use the $1/N$ expansion technique to generalize the results in Ref. [5] to arbitrary interactions and boson types. The analytic expression obtained for the transition matrix element is then used in a systematic study of medium-energy proton scattering from deformed nuclei in both the *sd* and *sdg* models.

## II. REVIEW OF THE EIKONAL APPROXIMATION AND THE IBM

Here, we briefly review and generalize the previous work done on the algebraic eikonal approach to medium-energy hadron-nucleus scattering (see [5] for details). The Hamiltonian for hadrons of mass $m$ scattering from a nucleus is given by

$$H=-\frac{\hbar^2}{2m}\nabla^2+H_{\rm IBM}+V_{\rm op}(\mathbf{r})+V_{\rm tr}(\mathbf{r},B)\ . \tag{2.1}$$

Here $\mathbf{r}$ is the projectile coordinate and $H_{\rm IBM}$ describes the collective excitations of the target nucleus. Introducing the boson operators $b_{lm}$, $l=0,2,4,\ldots,l_{\rm max}$, a general IBM Hamiltonian with one- and two-body terms can be written as

$$\begin{aligned} H_{\rm IBM}&=\sum_l \varepsilon_l n_l+\sum_{k=0}^{2l_{\rm max}}\kappa_k T^{(k)}\cdot T^{(k)}\ ,\\ n_l&=\sum_m b_{lm}^\dagger b_{lm}\ ,\\ T^{(k)}&=\sum_{jl} t_{kjl}[b_j^\dagger \tilde{b}_l]^{(k)}\ , \end{aligned} \tag{2.2}$$

where $n_l$ and $T^{(k)}$ are the boson number and multipole operators. The parameters consist of the single boson energies $\varepsilon_l$, the multipole strengths, and coefficients $\kappa_k$ and $t_{kjl}$, respectively. Of the two interaction terms in Eq.

 

(2.1), $V_{\rm op}(\mathbf{r})$ represents the optical potential that the projectile feels in the presence of the target. It is independent of the boson operators and hence cannot induce excitations in the target. A standard form for the optical potential is

$$V_{\rm op}(\mathbf{r})=-2\pi\hbar^2\frac{f}{m}\rho(r)\ , \tag{2.3}$$

where $f$ is the hadron-nucleon forward scattering amplitude, and $\rho(r)$ is the nuclear density (normalized to mass $A$) for which we take a two-parameter Fermi form

$$\rho(r)=\rho_0[1+e^{(r-R)/d}]^{-1}\ . \tag{2.4}$$

Finally, $V_{\rm tr}(\mathbf{r},B)$ in (2.1) represents the coupling between the projectile and the boson degrees of freedom generically denoted by $B$. It has the same form as Eq. (2.3) with $\rho(r)$ replaced by a hadronic transition density operator $\rho_{\rm tr}(\mathbf{r})$. With the usual assumption of one-body transition operators in the IBM, the spin zero density operator can be written as

$$\rho_{\rm tr}(\mathbf{r})=\sum_{kjl}\alpha_{kjl}(r)[b_j^\dagger\tilde{b}_l]^{(k)}\cdot Y^{(k)}(\hat{\mathbf{r}})\ . \tag{2.5}$$

Here, the $k$ sum runs over $k=2,4,\ldots,2l_{\rm max}$ dictated by the tensor properties of the boson operators and by the fact that the diagonal matrix element of $V_{\rm tr}(\mathbf{r},B)$ in the ground state should vanish as it is already contained in $V_{\rm op}(\mathbf{r})$. The quadrupole form factors $\alpha_{2jl}(r)$ in (2.5) have been determined from electron scattering experiments for various nuclei. The seniority breaking ($j\neq l$) form factors are surface peaked like the first derivative of the density (2.4), and the seniority conserving ones oscillate on the surface like the second derivative. In the absence of any other experimental information, we use the Tassie form factors [16] for all multipoles

$$\alpha_{kjl}(r)\equiv\alpha_k(r)\propto r^{k-1}\frac{d}{dr}\rho(r)\ ,\quad j\neq l\ , \tag{2.6a}$$

$$\alpha_{kjj}(r)\equiv\beta_k(r)\propto\frac{d}{dr}\alpha_k\ . \tag{2.6b}$$

Figure 1(a) shows typical quadrupole form factors obtained from (2.6). The normalizations of $\alpha_{kjl}(r)$ will be discussed in Sec. IV together with systematics. There are additional constraints on $\alpha_{kjl}(r)$ if the experimental $B(E\lambda)$ values are to be reproduced, e.g.,

$$B(E\lambda)=\frac{1}{4}\left|\int_0^\infty dr\, r^{\lambda+2}\langle J^\pi=\lambda^+\|\sum_{jl}\alpha_{\lambda jl}(r)[b_j^\dagger\tilde{b}_l]^{(\lambda)}\|0\rangle\right|^2\ , \tag{2.7}$$

where we assumed that hadronic form factors are twice as large as the electromagnetic ones. Equation (2.7) has an important ramification for the large $N$ behavior of the densities which will be used in the next section. Since the matrix elements of the boson multipole operators are proportional to $N$, the densities $\alpha_{kjl}$ should scale as $1/N$ to produce a finite $B(E\lambda)$ value in the large $N$ limit.

When the projectile energy is much larger than the interaction energies ($V_{\rm op}$ and $V_{\rm tr}$), so that its trajectory is little deflected from a straight line, one can use the eikonal approximation to describe the scattering. In addition, for medium-energy hadrons, one can neglect the nuclear excitation energies described by $H_{\rm IBM}$ in (2.1). Under these approximations, the scattering amplitude for the projectile going from momentum $\mathbf{k}_i$ to $\mathbf{k}_f$ while the nucleus is excited from an initial state $J_iM_i$ to a final state $J_fM_f$ is given by

$$A_{fi}(q)=\frac{k_i}{2\pi i}\int d^2b\, e^{i\mathbf{q}\cdot\mathbf{b}}\langle J_fM_f|e^{i\chi(\mathbf{b})}-1|J_iM_i\rangle\ , \tag{2.8}$$

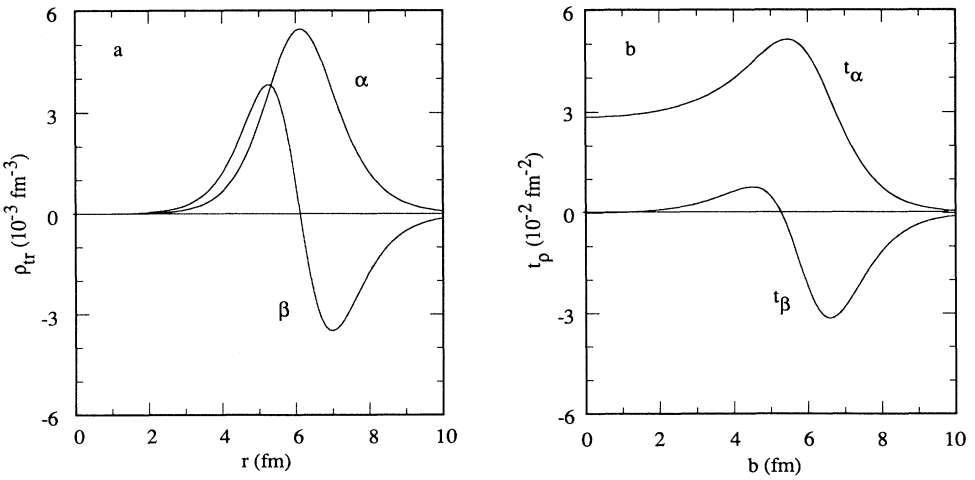


FIG. 1. (a) Form factors $\alpha_2(r)$ and $\beta_2(r)$ obtained from Eq. (2.6). The parameters of the Fermi density are $R=5.97$ and diffuseness $d=0.66$ fm. The normalizations are determined from experimental $B(E2)$ values as described in Sec. IV. (b) Profile functions $t_\alpha(b)$ and $t_\beta(b)$ for the form factors $\alpha_2(r)$ and $\beta_2(r)$.

where $\mathbf{q}=\mathbf{k}_f-\mathbf{k}_i$ is the momentum transfer, and $\chi(\mathbf{b})$ is the eikonal phase that the projectile acquires as it traverses the nucleus,

$$\chi(\mathbf{b})=-\frac{m}{\hbar^2 k_i}\int_{-\infty}^{\infty} dz[V_{\rm op}(\mathbf{r})+V_{\rm tr}(\mathbf{r},B)] . \quad (2.9)$$

Here, the $z$ axis is chosen along the incident beam direction $\hat{\mathbf{k}}$ so that the impact parameter $\mathbf{b}$ is perpendicular to $\hat{\mathbf{k}}$, i.e., $\mathbf{r}=\mathbf{b}+z\hat{\mathbf{k}}$. Since $V_{\rm op}$ is independent of the boson operators, it will be convenient to split $\chi(\mathbf{b})$ into two parts

$$\chi(\mathbf{b})=\bar{\chi}(b)+\hat{\chi}(\mathbf{b}) ,$$
$$\bar{\chi}(b)=\frac{2\pi f}{k_i}\int_{-\infty}^{\infty} dz\,\rho(r) , \quad (2.10)$$
$$\hat{\chi}(\mathbf{b})=\frac{2\pi f}{k_i}\int_{-\infty}^{\infty} dz\sum_{kjl}\alpha_{kjl}(r)[b_j^{\dagger}\tilde{b}_l]^{(k)}\cdot Y^{(k)}(\hat{\mathbf{r}}) ,$$

where $\bar{\chi}$ and $\hat{\chi}$ are the optical and transitional phases, and introduce the transition matrix element $U_{fi}$ as

$$U_{fi}=\langle J_f M_j|e^{i\hat{\chi}(\mathbf{b})}|J_i M_i\rangle . \quad (2.11)$$

The matrix element $U_{fi}$ can be greatly simplified by using the peripheral approximation $Y_m^{(k)}(\mathbf{r})\approx Y_m^{(k)}(\mathbf{b})$ in (2.10). This amounts to neglecting contributions from $(z/b)^2$ and higher-order terms in (2.10) which is justified for a surface interaction. Then the transition phase can be written as a rotation of a reduced transition phase $\hat{\chi}^{(0)}$ through the Euler angles $\hat{\mathbf{b}}=(\phi,\pi/2,0)$

$$\hat{\chi}(\mathbf{b})=R(\hat{\mathbf{b}})\hat{\chi}^{(0)}(b)R^{\dagger}(\hat{\mathbf{b}}) ,$$
$$\hat{\chi}^{(0)}(b)=\sum_{jlm}\phi_{jlm}(b)b_{jm}^{\dagger}b_{lm} , \quad (2.12)$$
$$\phi_{jlm}(b)=\frac{2\pi f}{k_i}(-1)^m\sum_k\left[\frac{2k+1}{4\pi}\right]^{1/2}\langle jml-m|k0\rangle \times\int_{-\infty}^{\infty} dz\,\alpha_{kjl}(r) .$$

From Eq. (2.6), the $b$ dependence of $\phi_{jlm}$ is described by the profile functions $t_{\alpha k}(b)=\int dz\,\alpha_k(r)$ and $t_{\beta k}(b)=\int dz\,\beta_k(r)$ which are shown in Fig. 1(b). Acting with the rotation operators on the nuclear states, the matrix element (2.11) becomes

$$U_{fi}=\sum_M D_{M_f M}^{(J_f)}(\hat{\mathbf{b}})D_{M_i M}^{(J_i)*}(\hat{\mathbf{b}})\langle J_f M|e^{i\hat{\chi}^{(0)}(b)}|J_i M\rangle . \quad (2.13)$$

Substituting (2.13) into (2.8), the azimuthal angle integration is given by the integral representation of the Bessel function $J_{|M_f-M_i|}$. Thus the scattering amplitude for excitation of a nucleus from the ground state ($J_i=M_i=0$) to a final state $J,M$ becomes

$$A_{fi}(q)=i^{M-1}k_i d_{M0}^{(J)}(\pi/2) \times\int_0^{\infty} b\,db\,J_M(qb)(e^{i\bar{\chi}}U_{fi}^{(0)}-\delta_{fi}) , \quad (2.14)$$

where we have introduced the reduced transition matrix $U_{fi}^{(0)}$

$$U_{fi}^{(0)}=\langle J0|e^{i\hat{\chi}^{(0)}(b)}|00\rangle , \quad (2.15)$$

which contains all the nuclear structure information. From a group theoretical view, the boson operators in (2.2) close under the group SU($n$), $n=\frac{1}{2}l_{\rm max}(l_{\rm max}+3)+1$, and the boson states form a basis for the symmetric irreducible representation of SU($n$) of rank $N$. Thus the transition operator in (2.15) is simply a transformation operator of SU($n$), and its matrix elements correspond to the representation matrix for this irreducible representation. In the next section, we show that $U_{fi}^{(0)}$ can be evaluated relatively easily using the $1/N$ expansion.

## III. TRANSITION MATRIX IN THE $1/N$ FORMALISM

The $1/N$ expansion is an angular momentum projected mean-field theory which provides analytic solutions for general IBM Hamiltonians with arbitrary kinds of bosons. The technique had been discussed in length elsewhere [14], and was shown to give an accurate representation of the low-lying collective bands when compared to the exact diagonalization results [15]. Since the details can be found in the literature, we do not consider it further here. (Some of the relevant formulas needed in the derivations are listed in Appendix A.) In this section, we use the $1/N$ expansion technique to evaluate the transition matrix (2.14).

For axially deformed systems, it is more convenient to work in the intrinsic frame. Introducing the intrinsic boson operator $b^{\dagger}=\sum_l x_l b_{l0}^{\dagger}$, the ground band can be written as a condensate of $N$ bosons

$$|\phi_g\rangle=\frac{1}{\sqrt{N!}}(b^{\dagger})^N|-\rangle . \quad (3.1)$$

Here $x_l$ are the normalized mean-field amplitudes which are determined from $H_{\rm IBM}$ by variation after projection. Going to the intrinsic frame breaks the rotational symmetry which has to be restored via angular momentum projection. Substituting (3.1) in (2.13) with the appropriate projection operators, the reduced transition matrix element becomes

$$U_{fi}^{(0)}=\frac{2J+1}{(8\pi^2)^2[\mathcal{N}_g(J)\mathcal{N}_g(0)]^{1/2}}\int d\Omega\,d\Omega' D_{00}^{(J)}(\Omega)\langle -|b^N R^{\dagger}(\Omega)e^{i\hat{\chi}^{(0)}}R(\Omega')(b^{\dagger})^N|-\rangle , \quad (3.2)$$

where the normalization $\mathcal{N}_g(J)$,

$$\mathcal{N}_g(J)=\frac{2J+1}{8\pi^2}\int d\Omega\, D^{(J)}_{00}(\Omega)\langle -|b^N R(\Omega)(b^\dagger)^N|-\rangle \ , \tag{3.3}$$

had been calculated previously as a $1/N$ expansion [see Eq. (A1)].

To evaluate the matrix element in (3.2), we need to know the effect of rotations and SU($n$) transformations on a single boson operator (i.e., the representation matrix). For rotations, this is given by Wigner $D$ matrices

$$R(\Omega)b^\dagger_{lm}R^\dagger(\Omega)=\sum_{m'} D^{(J)}_{m'm}(\Omega)b^\dagger_{lm'} \ . \tag{3.4}$$

Similarly, for the special SU($n$) transformation in (3.2), one can write

$$e^{i\hat{\chi}^{(0)}}b^\dagger_{lm}e^{-i\hat{\chi}^{(0)}}=\sum_{l'} U^{(m)}_{l'l}b^\dagger_{l'm} \ , \tag{3.5}$$

where $U^{(m)}_{l'l}$ is the transformation matrix. It had been derived previously in the special case of SU(6) [5]. Here we give a derivation for a general SU($n$) group. First, consider the eigenbosons of the transition phase $\hat{\chi}^{(0)}$

$$B^\dagger_m=\sum_l y_{lm}b^\dagger_{lm} \ , \tag{3.6}$$

which satisfies

$$[\hat{\chi}^{(0)},B^\dagger_m]=e_m B^\dagger_m \ . \tag{3.7}$$

Substituting (2.11) and (3.6) into (3.7), and working out the commutator leads to the eigenvalue equation

$$\sum_l \phi_{jlm}y_{lm}=e_m y_{jm} \ , \tag{3.8}$$

which determines the set of eigenvalues and eigenvectors $e^v_m$, $\{y^v_{lm}\}$, where $v$ is an index denoting different solutions. The order of the eigenvalue equation in (3.8) depends on $l_{\max}$ and $m$. For example, in the *sd* model, it has order 2 for $m=0$, and order 1 for $m=1,2$. In the *sdg* model, the order becomes 3 for $m=0$; 2 for $m=1,2$; and 1 for $m=3,4$. Thus the solution of (3.8) is trivial in the *sd* model and can be easily accomplished in the *sdg* model.

To make the connection with the transformation matrix, we next consider transformation of eigenbosons under SU($n$). It can be easily shown from (3.7) that the eigenbosons simply acquire a phase

$$e^{i\hat{\chi}^{(0)}}B^\dagger_m e^{-i\hat{\chi}^{(0)}}=e^{ie_m}B^\dagger_m \ . \tag{3.9}$$

Substituting (3.6) into (3.9) and using (3.5), we obtain

$$\sum_{l'} U^{(m)}_{ll'}y^v_{l'm}=e^{ie^v_m}y^v_{lm} \ , \quad \forall v \ , \tag{3.10}$$

which can be solved to yield for the transformation matrix

$$U^{(m)}_{ll'}=\sum_v e^{ie^v_m}y^v_{lm}y^v_{l'm} \ . \tag{3.11}$$

Transformation for $N$ boson operators follow from that of a single one through the relationship

$$U(b^\dagger_{lm})^N U^{-1}=(Ub^\dagger_{lm}U^{-1})^N \ . \tag{3.12}$$

Equipped with the transformation properties of the boson operators, Eqs. (3.4)–(3.5), the matrix element in (3.2) can now be easily evaluated using boson calculus,

$$\langle -|b^N R^\dagger(\Omega)e^{i\hat{\chi}^{(0)}}R(\Omega')(b^\dagger)^N|-\rangle=\Big[\sum_{ll'm} x_l x_{l'} D^{(l')*}_{m0}(\Omega)U^{(m)}_{l'l}D^{(l)}_{m0}(\Omega')\Big]^N$$
$$\equiv[f(\Omega,\Omega')]^N \ . \tag{3.13}$$

Substituting the $D$ matrices and $U^{(m)}_{l'l}$ (3.11) into (3.13), we obtain a particularly simple form for $f$,

$$f(\theta,\phi,\theta',\phi')=\sum_m e^{im(\phi-\phi')}\sum_v e^{ie^v_m}f^v_m(\theta)f^v_m(\theta') \ ,$$
$$f^v_m(\theta)=\sum_l x_l y^v_{lm}d^{(l)}_{m0}(\theta) \ , \tag{3.14}$$

and the transition matrix (3.2) becomes

$$U^{(0)}_{fi}=\frac{2J+1}{(4\pi)^2[\mathcal{N}_g(J)\mathcal{N}_g(0)]^{1/2}}\int \sin\theta\, d\theta\, d\phi \sin\theta'\, d\theta' d\phi' P_J(\cos\theta)[f(\theta,\phi,\theta',\phi')]^N \ . \tag{3.15}$$

Since the $\phi$ integrals in (3.15) involve the difference $\phi-\phi'$, one of them is trivial and gives $2\pi$ after a coordinate transformation. This leaves a three-dimensional integral behind which can be evaluated numerically. Our aim here, however, is to use a large $N$ expansion for the integrand in (3.15) and obtain an analytical expression for the transition matrix.

The standard technique for approximating integrals of the form (3.15) is the method of steepest descent which gives the leading-order term (in $N$) correctly, and hence it is especially good for large $N$. This method exploits the fact that the main contribution to the integral comes from the region where $f$ has a maximum. At the maximum, $f^N$ is approximated by a Gaussian and the result-

ing integral can be evaluated without difficulty. To find the extremum points, consider the derivatives of $f(\theta,\theta',\phi)$,

$$\frac{\partial f}{\partial\theta}=\sum_m e^{im\phi}\sum_v e^{ie_m^v}f_m^v(\theta')\frac{\partial f_m^v(\theta)}{\partial\theta}=0\ , \tag{3.16a}$$

$$\frac{\partial f}{\partial\theta'}=\sum_m e^{im\phi}\sum_v e^{ie_m^v}f_m^v(\theta)\frac{\partial f_m^v(\theta')}{\partial\theta'}=0\ , \tag{3.16b}$$

$$\frac{\partial f}{\partial\phi}=i\sum_m me^{im\phi}\sum_v e^{ie_m^v}f_m^v(\theta)f_m^v(\theta')=0\ , \tag{3.16c}$$

which should vanish simultaneously. From the symmetry of $f(\theta,\theta',\phi)$ with respect to $\theta\leftrightarrow\theta'$, it is clear that $\theta=\theta'$ at the maximum. Thus, to satisfy (3.16a) and (3.16b), either $f_m^v(\theta)$ (3.14) or its derivative should vanish for all $m$ and $v$. Noticing that $f_m^v(\theta)$ involves an arbitrary sum of the $d$ functions with different weights for each $m$ and $v$, this would be possible only if the $d$ function or its derivatives vanish simultaneously for each $l$. Common zeros of the $d$ functions and its derivatives occur only at $\theta=0$, $\pi/2$, $\pi$ (see Table I). Since $f(\theta,\theta',\phi)$ has the same value at $\theta=0$ and $\pi$, it is sufficient to consider only one of them. Inspection of Table I shows the following. (i) For $\theta=\theta'=0$, Eqs. (3.16) are satisfied irrespective of the value of $\phi$. However, all the second derivatives involving $\phi$ and hence the Hessian of $f$ also vanish at this point. Therefore it is not a maximum and not likely to contribute to the integral. To see this more explicitly consider

$$f(0,0,\phi)=\sum_v e^{ie_0^v}\left[\sum_l x_l y_{l0}^v\right]^2\ , \tag{3.17}$$

which can be estimated using $y_{l0}^1\approx x_l$. Then, from the orthogonality of the eigenvectors, only the $v=1$ term contributes to the sum in (3.17). Since $e_0^1$ is the largest (positive) root and predominantly imaginary, $f(0,0,\phi)\approx\exp(ie_0^1)<1$, and $[f(0,0,\phi)]^N\to 0$ for large $N$. (ii) For $\theta=\theta'=\pi/2$, Eqs. (3.16) are satisfied when $\sin 2\phi=0$, i.e., $\phi=0$, $\pi/2$, $\pi$, $3\pi/2$, $2\pi$. At $\phi=\pi/2$ and $3\pi/2$, the second derivative of $f$ with respect to $\phi$ and its Hessian are positive hence they correspond to the minima of $f$. For the other values of $\phi$, the reverse is true, and these are the maxima of $f$ needed in the calculation. In fact, using $[-\pi/2,\ 3\pi/2]$ for the $\phi$ integral limits instead of $[0,2\pi]$ to avoid the maximums at the end points, there are only two maxima of $f$ at $\phi=0$ and $\pi$ making equal contributions to the integral.

In evaluating the integral it is more convenient to use the variable $z=\cos\theta$. Since the first and second derivatives of $d_m^{(l)}$ (and hence $f$) with respect to $\theta$ and $z$ are the same at $\theta=\pi/2$, $f^N$ has the same Gaussian form with respect to either variables. The nonvanishing second derivatives of $f(z,z',\phi)$ at $z=z'=\phi=0$ are given by

$$f_0\equiv f(0,0,0)=\sum_{\substack{\text{even } m\\ v}} e^{ie_m^v}\left[\sum_l c_{lm}x_l y_{lm}^v\right]^2\ , \tag{3.18a}$$

$$f_1\equiv\frac{1}{f_0}\frac{\partial^2 f}{\partial z\,\partial z'}\bigg|_{(0,0,0)}=\frac{1}{f_0}\sum_{\substack{\text{odd } m\\ v}} e^{ie_m^v}\left[\sum_l\frac{1}{c_{lm}}x_l y_{lm}^v\right]^2\ , \tag{3.18b}$$

$$f_2\equiv-\frac{1}{f_0}\frac{\partial^2 f}{\partial z^2}\bigg|_{(0,0,0)}=\frac{1}{f_0}\sum_{\substack{\text{even } m\\ v}} e^{ie_m^v}\left[\sum_l(\bar{l}-m^2)c_{lm}x_l y_{lm}^v\right]\left[\sum_{l'}c_{l'm}x_{l'}y_{l'm}^v\right]\ , \tag{3.18c}$$

$$f_3\equiv-\frac{1}{f_0}\frac{\partial^2 f}{\partial\phi^2}\bigg|_{(0,0,0)}=\frac{1}{f_0}\sum_{\substack{\text{even } m\\ v}} m^2 e^{ie_m^v}\left[\sum_l c_{lm}x_l y_{lm}^v\right]^2\ , \tag{3.18d}$$

where the coefficients $c_{lm}$ follow from Table I as

$$c_{lm}=(-1)^{1/2}\frac{\sqrt{(l-m)!(l+m)!}}{(l-m)!!(l+m)!!}\ . \tag{3.19}$$

Using the method of steepest descent with Eq. (3.18), the integral in (3.15) can now be approximated as

TABLE I. Special values of the $d$ functions and its derivatives for $\theta=0$ and $\pi/2$ [17].

| | $\theta=0$ | $\theta=\pi/2$ |
|---|---|---|
| $d_{m0}^{(l)}(\theta)$ | $\delta_{m0}$ | $(-1)^{(l+m)/2}\frac{\sqrt{(l-m)!(l+m)!}}{(l-m)!!(l+m)!!}\delta_{l+m\ \text{even}}$ |
| $\frac{d}{d\theta}d_{m0}^{(l)}(\theta)$ | $\frac{1}{2}\sqrt{\bar{l}}(\delta_{m-1}-\delta_{m1})$ | $(-1)^{(l+m+1)/2}\frac{(l-m)!!(l+m)!!}{\sqrt{(l-m)!(l+m)!}}\delta_{l+m\ \text{odd}}$ |
| $\frac{d^2}{d\theta^2}d_{m0}^{(l)}(\theta)$ | $-\frac{1}{2}\bar{l}\delta_{m0}+\frac{1}{4}\sqrt{\bar{l}(\bar{l}-2)}\delta_{m\pm2}$ | $-(\bar{l}-m^2)d_{m0}^{(l)}$ |

$$I=4\pi\int_{-1}^{1}dz\int_{-1}^{1}dz'\int_{-\pi/2}^{\pi/2}d\phi\,P_J(z)f_0^N\exp\{-\tfrac{1}{2}N(f_2z^2-2f_1zz'+f_2z'^2+f_3\phi^2)\}\ . \tag{3.20}$$

For large $N$, the limits of the $\phi$ and $z'$ integrals can be extended to $\pm\infty$. The resulting Gaussian integrals are standard and give

$$I=\frac{8\pi^2}{N}\frac{f_0^N}{(f_2f_3)^{1/2}}\int_{-1}^{1}dz\,P_J(z)\exp\{gz^2\}\ ,\quad g=-\tfrac{1}{2}Nf_2(1-f_1^2/f_2^2)\ . \tag{3.21}$$

Care needs to be exercised in evaluating the $z$ integral in (3.21), as the limits cannot be extended to $\pm\infty$ in this case. This happens because $f_1/f_2$ has a $1/N$ expansion whose leading term is 1 (see Appendix B), and hence $g$ in (3.21) is neither large nor is it clearly negative. An exact evaluation can nevertheless be carried out by expanding the exponential and integrating the powers of $z$ using the result [18]

$$\int_{-1}^{1}dz\,z^{2n}P_J(z)=\begin{cases}0\ , & \text{if } n<J/2\\ \dfrac{2^{-J}(2n)!\Gamma(n-J/2+\frac{1}{2})}{(2n-J)!\Gamma(n+J/2+\frac{3}{2})}\ , & \text{if } n\geq J/2\end{cases}\ . \tag{3.22}$$

It is clear from (3.22) that the first nonzero term in the expansion comes from $n=J/2$. Factoring out this term, the remaining series is given by the confluent hypergeometric function, and the integral in (3.21) can be written in a closed form,

$$I=\frac{16\pi^2}{N}\frac{(J-1)!!}{(2J+1)!!}\frac{f_0^N}{(f_2f_3)^{1/2}}(2g)^{J/2}M(\tfrac{1}{2}(J+1),J+\tfrac{3}{2};g)\ . \tag{3.23}$$

Substituting the integral (3.23) into (3.15) and the leading-order normalizations from (A1), we obtain for the transition matrix

$$U_{fi}^{(0)}=\frac{a}{2}(2J+1)^{1/2}\frac{(J-1)!!}{(2J+1)!!}\frac{f_0^N}{(f_2f_3)^{1/2}}(2g)^{J/2}M(\tfrac{1}{2}(J+1),J+\tfrac{3}{2};g)\ , \tag{3.24}$$

where $M$ is a confluent hypergeometric function. Equation (3.24) has a similar functional dependence as the exact SU(3) result in the large $N$ limit [5]. In fact, as shown in Appendix B, substituting the SU(3) values in (3.24) reproduces that result. Note that so far we have ignored any Coulomb effects. In the final calculation of cross sections, we have included Coulomb scattering using the prescription given in Refs. [7] and [19].

## IV. SYSTEMATICS FOR DEFORMED NUCLEI

In this section, we use the results derived in Sec. IV to discuss the cross-section systematics for medium-energy (800 MeV) proton scattering from deformed nuclei in both the *sd* and *sdg* models. Specifically, we have rare-earth nuclei in mind, and use parameters typical of this region, e.g., the target nucleus has $A=160$ and $N=14$ bosons, Fermi distribution (2.4) has radius $R=1.1A^{1/3}$, and diffuseness $d=0.66$ fm, and the proton-nucleon forward scattering amplitude (2.3) is given by $f/k_i=\sigma(r+i)/4\pi$, $\sigma=41$ mb, $r=-0.17$. The normalizations of the form factors are determined from the electromagnetic multipole operators

$$T(E)=e_k\sum_{jl}t_{kjl}[b_j^\dagger\tilde{b}_l]^{(k)}\ , \tag{4.1}$$

by demanding

$$e_kt_{kjl}=\tfrac{1}{2}\int_0^\infty dr\,r^{k+2}\alpha_{kjl}(r)\ . \tag{4.2}$$

Here $e_k$ are the boson effective charges. Suitable choices for the multipole operators are discussed below for the individual cases. Finally, the mean fields for a given IBM Hamiltonian are determined through the variational principle as in Ref. [14], and listed in Table II for the particular cases used below.

### A. *sd* boson model

The *sd* IBM has been most successfully applied to the rare-earth region with the simple Hamiltonian

$$H=\kappa Q\cdot Q\ ,\quad Q=(s^\dagger\tilde{d}+d^\dagger s)+\chi(d^\dagger\tilde{d})^{(2)}\ , \tag{4.3}$$

and the $E2$ operator $T(E2)=e_2Q$ which is known in the literature as the consistent $Q$ formalism (CQF) [20]. Here, we use the CQF to describe proton scattering. The effective charges deduced from the experimental $B(E2)$

TABLE II. The *sd* (top rows) and *sdg* (bottom rows) mean fields used in the calculations.

| | $x_0$ | $x_2$ | $x_4$ |
|---|---|---|---|
| $\chi=0$ | $1/\sqrt{2}$ | $1/\sqrt{2}$ | . . . |
| $\chi=-\sqrt{7}/4$ | 0.643 | 0.766 | . . . |
| $\chi=-\sqrt{7}/2$ | $1/\sqrt{3}$ | $\sqrt{2}/\sqrt{3}$ | . . . |
| $q=0$ | 0.663 | 0.725 | 0.188 |
| $q=1/2$ | 0.592 | 0.772 | 0.230 |
| $q=1$ | 0.523 | 0.808 | 0.272 |

values are almost constant in the region which is taken as $e_2=0.13$ $e$ b. In Fig. 2, we show the effect of the $\chi$ parameter in (4.3) on cross sections for the $J=0$ and 2 states of the ground band. With increasing $\chi$, cross sections are enhanced which can be interpreted as due to larger deformations. Most of the rare-earth nuclei fall in the middle ($\chi=-\sqrt{7}/4$) which is represented by the dashed line.

We next consider the effect of the hexadecapole interaction using the same $E2$ charge and $\chi=-\sqrt{7}/4$. The hexadecapole operator in the $sd$ model, $T(E4)=e_4(d^\dagger\tilde{d})^{(4)}$, is an effective operator and should be used with care. Since it is seniority conserving, one would expect to use an oscillating form factor (2.6b). However, experimentally it is found to have a surface peaked form factor, and therefore we choose to use the form (2.6a) in the following. The $E4(0_1\rightarrow 4_1)$ matrix elements follow a sinelike curve in the rare-earth region, changing sign in the middle of the 50–82 shell. Such a variation follows from a microscopic mapping of the boson Hamiltonian [21]. Here, we implement it phenomenologically by varying $e_4$ in the range $[-0.05,+0.05]$ $e$ b$^2$ which roughly covers the $E4$ data. Figure 3 shows cross sections for the $J=0$, 2, and 4 states of the ground band for different choices of the hexadecapole strength. Apart from a slight shift to the right with increasing $E4$ strength [which is due to the different $r$ dependence in the $E2$ and $E4$ form factors (2.6a)], the cross sections basically retain their shapes. This means that one can simulate the effect of the $E4$ operator by simply adjusting the $E2$ strengths. In other words, the effective $E4$ operator in the $sd$ model does not contain any new information. An interesting side remark here is the opposite behavior of the interference patterns for the elastic and inelastic scattering which is constructive for the former and destructive for the latter when the interactions have the same signs (the reverse is true for different signs). Although the influence of the hexadecapole interaction diminishes with decreasing spin, it is appreciable enough even for the $J=0$ state which necessitates simultaneous description of cross sections for all states.

### B. *sdg* boson model

A pure quadrupole form for the Hamiltonian as in (4.3) leads to a too strong coupling of $g$ bosons at variance with experiment. We therefore modify (4.3) by adding a one-body $g$ boson energy with $\epsilon_g=1$ MeV, which gives a similar description of the low-lying levels as in the $sd$ model with the same $\kappa$ ($-20$ keV). The quadrupole and hexadecapole operators are replaced by

$$\begin{aligned} Q&=(s^\dagger\tilde{d}+d^\dagger s)+q_{22}(d^\dagger\tilde{d})^{(2)} \\ &\quad+q_{24}(d^\dagger\tilde{g}+g^\dagger\tilde{d})^{(2)}+q_{44}(g^\dagger\tilde{g})^{(2)}\ , \\ T^{(4)}&=(s^\dagger\tilde{g}+g^\dagger s)+h_{22}(d^\dagger\tilde{d})^{(4)} \\ &\quad+h_{24}(d^\dagger\tilde{g}+g^\dagger\tilde{d})^{(4)}+h_{44}(g^\dagger\tilde{g})^{(4)}\ . \end{aligned} \tag{4.4}$$

Due to renormalization, one needs smaller effective charges in the $sdg$ model. In order to obtain the same matrix elements as in the $sd$ model, we use in the following $e_2=0.113$. $e$ b, and vary $e_4$ in the range $[-0.028,+0.028]$ $e$ b$^2$. In the SU(3) limit, the quadrupole parameters are given by $(q_{22},q_{24},q_{44})=(-1.242,1.286,-1.589)$. It was shown in Refs. [14,15] that by weighting the SU(3) values with $(q,1,q)$ where $q$ varies in the range [0,1], one can mimic the $sd$ model results with a variable $\chi$; that is, the parameter $q$ here plays the role of $\chi$. That this similarity in static properties is also carried to proton scattering is demonstrated in Fig. 4 which shows cross sections for the $J=0$ and 2 states of the ground band for $q=0$ ($\gamma$-unstable limit), $q=\frac{1}{2}$ (intermediate), and $q=1$ [SU(3) limit]: the curves in Figs. 2 and 4 almost overlap. This result persists even for scattering to higher spin states (e.g., Fig. 7), indicating that renormalization of $g$ boson effects, which is known to hold for static quadrupole properties [22],

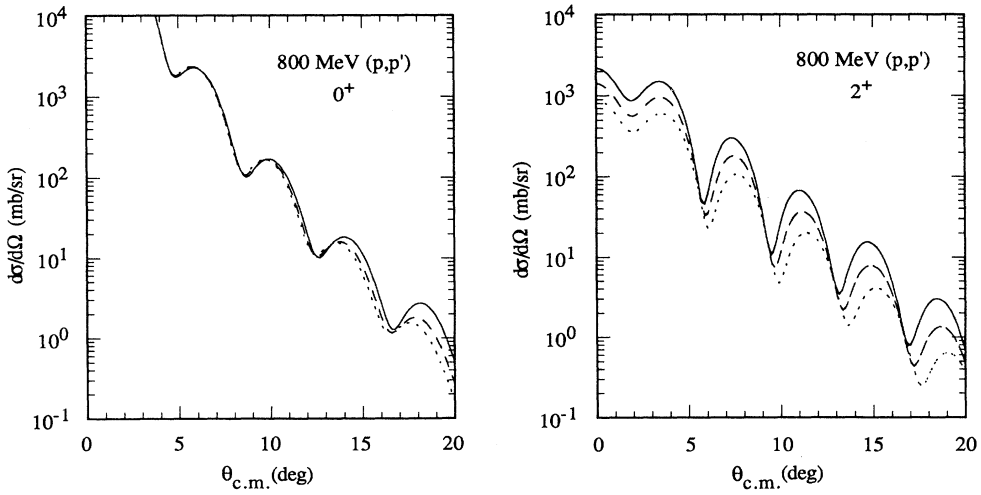


FIG. 2. Effect of the $\chi$ parameter in the quadrupole operator on cross sections for the $J=0$ and 2 states of the ground band. The solid and dotted lines correspond to the SU(3) ($\chi=-\sqrt{7}/2$) and O(6) ($\chi=0$) limits, and the dashed line to a midvalue ($\chi=-\sqrt{7}/4$).

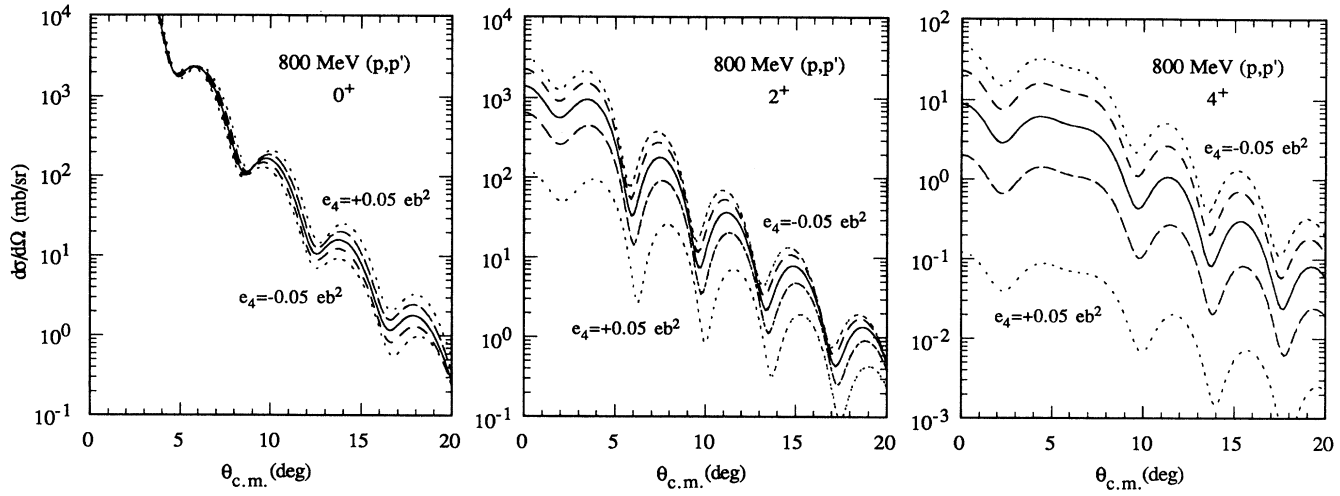


FIG. 3. Effect of the hexadecapole interaction on cross section for the $J=0$, 2, and 4 states of the ground band. The solid line is for $e_4=0$ (quadrupole interaction only), and the dashed and dotted lines are for $e_4=\pm 0.025\ e\,b^2$ and $e_4=\pm 0.05\ e\,b^2$, respectively. The direction of increasing $e_4$ is indicated.

also extends to dynamic properties.

The choice of the $E4$ operator is more complicated due to lack of data. A contending choice for deformed nuclei is to determine it from the $E2$ operator through a commutation relation which ensures coherence of the quadrupole and hexadecapole mean fields [23]. This approach yields for $h_{ij}$ in (4.4)

$$\bar{h}_{22}=\bar{q}_{24}\ ,\quad \bar{h}_{24}=\bar{q}_{44}\ ,\quad \bar{h}_{44}=\bar{q}_{24}+(\bar{q}_{44}^2-\bar{q}_{22}\bar{q}_{44}-1)/\bar{q}_{24}\ , \tag{4.5}$$

where $\bar{q}_{jl}=\langle j0l0|20\rangle q_{jl}$, $\bar{h}_{jl}=\langle j0l0|40\rangle h_{jl}$. The resulting values for $q=\frac{1}{2}$ together with the SU(3) (2,2) tensor operator and its scaling with $(\frac{1}{2},1,\frac{1}{2})$ similar to the quadrupole operator are shown in Table III. The $e_4$ values are chosen to given the same $B(E4)$ value. As in the *sd* model, we keep the same $E2$ charge and use $q=\frac{1}{2}$ when including the hexadecapole interaction. Figure 5 shows the effect of the coherent choice of the $E4$ operator on cross sections for the $J=0$, 2, and 4 states of the ground band (in order to avoid cluttering, we do not show any intermediate $e_4$ values here). Comparing Figs. 3 and 5, we get a completely different picture. The $E4$ operator in the *sdg* model contains new information whose effects cannot be simulated by changing the $E2$ strengths. Other remarks made for the *sd* model concerning the interference pattern and the necessity of simultaneous fits remain same (even reinforced). The effect of different $E4$ operators (Table III) on cross sections is demonstrated in Fig. 6. The cross sections are slightly shifted which indicates that by adjusting the $E4$ strength one can obtain similar results for widely differing $E4$ operators. Thus the structure of the $E4$ operator can only be resolved by measuring the excitation cross sections for the side bands.

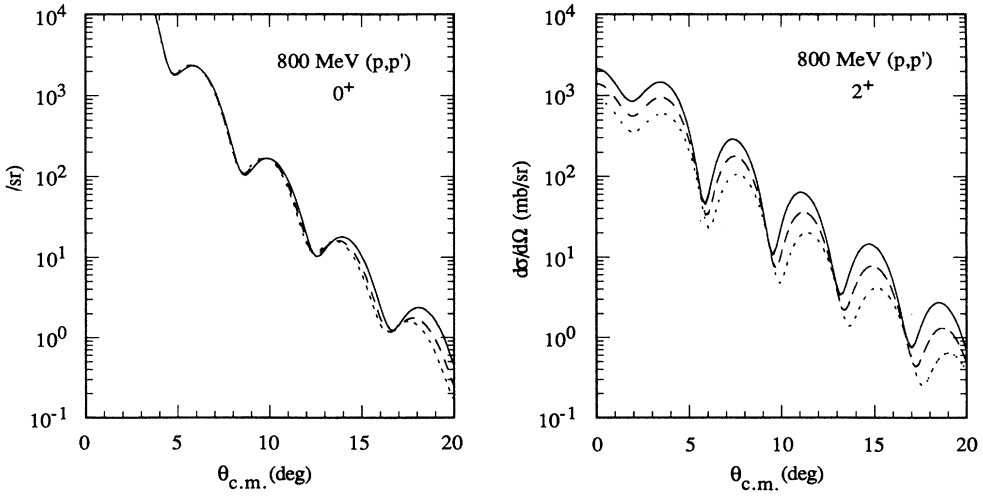


FIG. 4. Same as in Fig. 2 but in the *sdg* boson model. The solid line corresponds to the SU(3) quadrupole interaction, and the dotted line to the $\gamma$-unstable limit. The dashed line shows an intermediate situation.

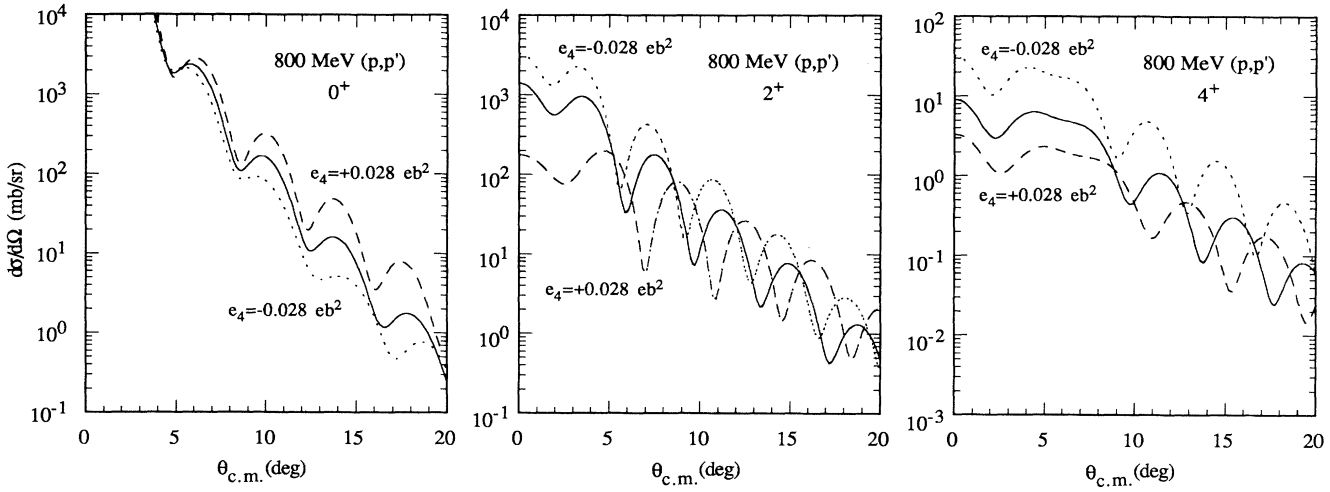


FIG. 5. Same as in Fig. 3 but in the *sdg* boson model. The solid line is for $e_4=0$, the dotted one for $e_4=-0.028\ e\ \mathrm{b}^2$ and dashed one for $e_4=+0.028\ e\ \mathrm{b}^2$.

Finally, Fig. 7 shows cross sections for the excitation of the first $6^+$ state in both the *sd* and *sdg* models. In the *sd* model, contrary to the *sdg* model (and experiment), inclusion of the hexadecapole interaction leads to a very sharp drop in the cross section which suggests that the effective $E4$ operator in *sd* model may have a very limited usage.

## V. SUMMARY AND CONCLUSIONS

The $1/N$ expansion provides approximate analytic solutions for general IBM Hamiltonians with arbitrary kinds of bosons. It had previously been applied to a variety of nuclear structure problems, and proven especially useful for the *sdg* model where numerical diagonalization is difficult due to large basis space. In this work, we have extended its application to medium-energy hadron-nucleus scattering in the algebraic eikonal framework, deriving a general analytic expression for the transition matrix accurate to leading order in $N$.

Using this result, we have made a systematic study of proton scattering from deformed nuclei contrasting the behavior of the *sd* and *sdg* models. The main conclusions emerging from this study are (i) the quadrupole interaction leads to almost identical cross sections in both models indicating that renormalization of the *g* boson is also valid for dynamical quadrupole properties, and (ii) the hexadecapole interaction gives very different results suggesting that the effective $E4$ operator used in the *sd* model cannot describe the hexadecapole properties adequately.

We have not presented any applications to specific nuclei here because data exist for scattering to $J=4^+$ states only for the ground band (more extensive data exist for the $J=2^+$ states but they have already been well analyzed [7,8]). It is clear from the last section that study of the ground band $J=4$ state alone is not very informative

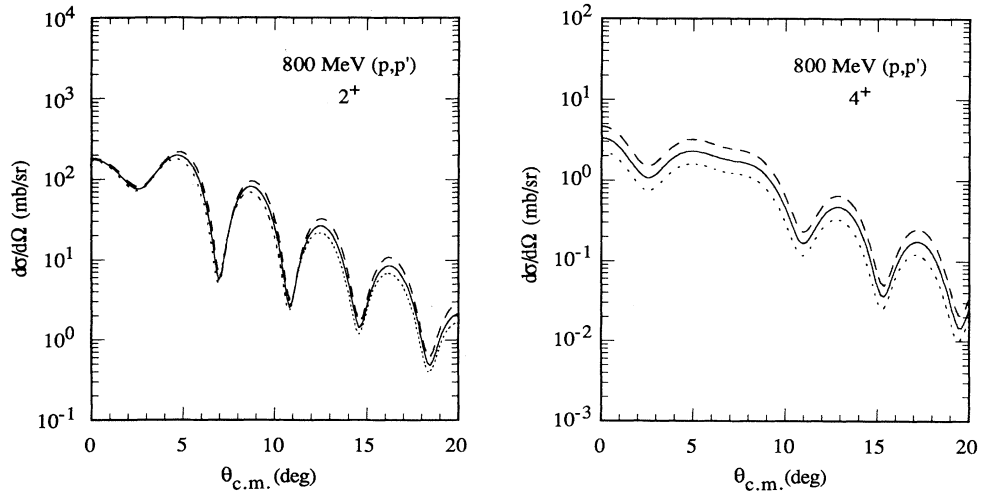


FIG. 6. Influence of the different choices for the hexadecapole operator on scattering cross sections for $J=2$ and 4 states of the ground band. The solid line represents the coherent hexadecapole operator, the dashed and dotted lines correspond to the SU(3) (2,2) tensor and its scaling, respectively.

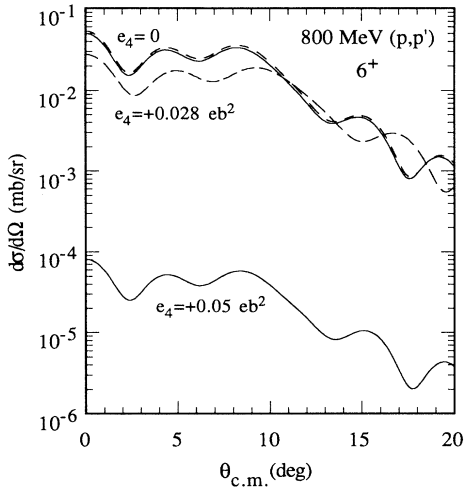


FIG. 7. Cross sections for excitation of the first $6^+$ state in the *sd* (solid lines) and the *sdg* (dashed lines) models with ($e_4>0$) and without ($e_4=0$) hexadecapole interaction.

as almost any choice for the $E4$ operator gives similar results (Fig. 6). Theoretical calculation of cross sections for excitation of the side bands, along the lines presented in this paper, is in progress. We therefore urge for experimental study of higher-lying $J=4^+$ states in deformed nuclei via medium-energy proton scattering.

Finally, we emphasize the simplicity of the results compared to the coupled-channel method. The main computational effort here is the numerical evaluation of one-dimensional integrals which takes a few seconds of CPU on a VAX computer. A similar coupled-channel calculation would take hours. Thus the $1/N$ formalism would be especially useful in a parameter search situation where calculations had to be repeated many times.

The $1/N$ expansion technique has already been applied to sub-barrier fusion [24] with matching advantages over the coupled-channel method. Plans are also underway to use it in electron-molecule scattering which had been treated previously in the algebraic eikonal approach using the dynamical symmetries [25].

## ACKNOWLEDGMENTS

S.K. would like to thank Dr. J. Ginocchio for his hospitality and useful discussions at the Los Alamos National Laboratory where part of this work was carried out. This work is supported by the Australian Research Council.

## APPENDIX A

The integral in Eq. (3.3) is basic to the $1/N$ expansion technique, and appears in the evaluation of all matrix elements. It is given in the form of a double expansion in $1/N$ and $\bar{J}=J(J+1)$ [14,15]

TABLE III. Parameters $e_4$ and $h_{jl}$ for different choices of the hexadecapole operator.

| | $e_4$ ($e$ b$^2$) | $h_{22}$ | $h_{24}$ | $h_{44}$ |
|---|---|---|---|---|
| Coherent | 0.028 | 0.958 | −0.592 | −1.942 |
| SU(3) (2,2) | 0.018 | 1.517 | −1.185 | 1.281 |
| Scaled SU(3) | 0.025 | 0.759 | −1.185 | 0.641 |

$$\mathcal{N}_g(J)=\frac{2J+1}{aN}\left[1-\frac{1}{aN}(\bar{J}+a_1)+\frac{1}{2!(aN)^2}(\bar{J}^2+\alpha_2\bar{J}+\alpha_2')-\cdots\right], \quad \text{(A1)}$$

where the coefficients $\alpha_i$ are defined in terms of the moments of the mean fields $a_n$ [$a\equiv a_0$, $\bar{l}=l(l+1)$]

$$a_n=\sum_l \bar{l}^{n+1}x_l^2 , \quad \text{(A2)}$$

as $\alpha_1=a+1-a_1/a$, $\alpha_2=6\alpha_1-2$, etc.

## APPENDIX B

The coefficients $f_i$ (3.18) can be expanded in $1/N$ as

$$f_i=\sum_{n-0}^{\infty} f_i^{(n)}/N^n . \quad \text{(B1)}$$

Here, we derive the leading-order terms $f_i^{(0)}$ in (B1) which are obtained from (3.18) by replacing the exponentials with 1. Using the closure relation $\sum_v y_{lm}^v y_{l'm}^v=\delta_{ll'}$ and the identities obtained from the properties of the $d$ functions [17]

$$\sum_{\text{even } m}(c_{lm})^2=1 , \quad \sum_{\text{odd } m}(1/c_{lm})^2=\tfrac{1}{2}\bar{l} , \quad \sum_{\text{even } m}(mc_{lm})^2=\tfrac{1}{2}\bar{l} , \quad \text{(B2)}$$

the sums over $v$ and $m$ can be done yielding

$$f_0^{(0)}=1 , \quad f_1^{(0)}=f_2^{(0)}=f_3^{(0)}=\tfrac{1}{2}\sum_l \bar{l}x_l^2=\tfrac{1}{2}a , \quad \text{(B3)}$$

which proves that $g$ in Eq. (3.21) has a vanishing leading-order term.

In the SU(3) limit, assuming identical form factors for the *sd* and *dd* terms, the eigenvalue equations (3.8) gives

$$\begin{aligned} &y_{00}^1=1/\sqrt{3} , \quad y_{20}^1=\sqrt{2/3} , \quad e_0^1=\sqrt{2}\phi_{200} , \\ &y_{00}^2=\sqrt{2/3} , \quad y_{20}^2=-1/\sqrt{3} , \quad e_0^2=-\tfrac{1}{2}e_0^1 , \\ &y_{21}^1=1 , \quad e_1^1=\tfrac{1}{4}e_0^1 , \\ &y_{22}^1=1 , \quad e_2^1=-\tfrac{1}{2}e_0^1 . \end{aligned} \quad \text{(B4)}$$

The second derivatives in (3.18) become

$$f_0=\exp(ie_0^2)\ ,\quad f_1=2\exp(ie_1^1)/f_0\ ,\quad f_2=f_3=2\ . \tag{B5}$$

Introducing $\bar{g}=-i\sqrt{2}N\phi_{200}$ as in [5], $g$ in (3.21) becomes $g=-3\bar{g}/2$ leading order in $N$. Finally, substituting these values into (3.24), we obtain

$$U_{fi}^{(0)}=(2J+1)^{1/2}\frac{(J-1)!!}{(2J+1)!!}(-3\bar{g})^{J/2} \times e^{\bar{g}/2}M(\tfrac{1}{2}(J+1),J+\tfrac{3}{2};-\tfrac{3}{2}\bar{g})\ , \tag{B6}$$

which agrees with Eq. (9.6a) of Ref. [5].


[1] M. L. Barlett *et al.*, Phys. Rev. C **22**, 408 (1980).
[2] R. D. Amado, J. P. Dedonder, and F. Lenz, Phys. Rev. C **21**, 647 (1980).
[3] R. J. Glauber, in *Lectures in Theoretical Physics,* edited by W. E. Brittin and L. G. Dunham (Interscience, New York, 1959), Vol. 1, p. 315.
[4] R. D. Amado, Adv. Nucl. Phys. **15**, 1 (1985).
[5] J. N. Ginocchio, T. Otsuka, R. D. Amado, and D. A. Sparrow, Phys. Rev. C **33**, 247 (1986).
[6] F. Iachello and A. Arima, *The Interacting Boson Model* (Cambridge University Press, Cambridge, 1987).
[7] G. Wenes, J. N. Ginocchio, A. E. L. Dieperink, and B. van der Cammen, Nucl. Phys. **A459**, 631 (1986).
[8] J. N. Ginocchio *et al.*, Phys. Rev. C **36**, 2436 (1987).
[9] G. Wenes and J. N. Ginocchio, J. Phys. G **14**, S65 (1988).
[10] W. Boeglin *et al.*, Nucl. Phys. **A477**, 399 (1988), and references therein.
[11] A. Sethi *et al.*, Phys. Rev. C **44**, 700 (1991), and references therein.
[12] N. Yoshinaga, Y. Akiyama, and A. Arima, Phys. Rev. C **38**, 419 (1988).
[13] S. Kuyucak, V-S. Lac, I. Morrison, and B. R. Barrett, Phys. Lett. B **263**, 347 (1991); V.-S. Lac and S. Kuyucak, Nucl. Phys. **A539**, 418 (1992).
[14] S. Kuyucak and I. Morrison, Ann. Phys. (N.Y.) **181**, 79 (1988); **195**, 126 (1989).
[15] S. Kuyucak and I. Morrison, Phys. Rev. C **41**, 1803 (1990).
[16] L. J. Tassie, Aust. J. Phys. **9**, 407 (1956).
[17] D. A. Varshalovich, A. N. Moskalev, and V. K. Khersonskii, *Quantum Theory of Angular Momentum* (World Scientific, Singapore, 1988).
[18] I. S. Gradshteyn and I. M. Ryzhik, *Tables of Integrals, Series and Products* (Academic, New York, 1980).
[19] R. M. Ikeda and J. A. McNeil, Phys. Rev. C **24**, 2754 (1981).
[20] R. F. Casten and D. D. Warner, Rev. Mod. Phys. **60**, 389 (1988).
[21] I. Morrison, J. Phys. G **12**, L201 (1986).
[22] T. Otsuka and J. N. Ginocchio, Phys. Rev. Lett. **55**, 276 (1985).
[23] S. Kuyucak, I. Morrison, and T. Sebe, Phys. Rev. C **43**, 1187 (1991).
[24] A. B. Balantekin, J. R. Bennett, A. J. DeWeerd, and S. Kuyucak Phys. Rev. C **46**, 2019 (1992).
[25] R. Bijker, R. D. Amado, and D. A. Sparrow, Phys. Rev. A **33**, 871 (1986).